

Supporting information

Amines-induced Phase Transition from White Phosphorus to Red/Black Phosphorus for Li/K-ion Storage

*Yang Li, Song Jiang, Yong Qian, Ying Han, Jie Zhou, Tieqiang Li, Longchang Xi,
Ning Lin*, Yitai Qian*
*Department of Applied Chemistry, School of Chemistry and Materials Science,
University of Science and Technology of China, Hefei 230026, China*
E-mail: ningl@mail.ustc.edu.cn

Experimental Section

1.1 Materials

White phosphorus was purchased from DAMAO Chemical Reagent Factory, N,N'-dimethylethylenediamine was purchased from Shanghai Xianding Biochemical Technology Co. Ltd., N,N,N',N'-tetramethylethylenediamine was purchased from Shanghai Aladdin Biochemical Technology Co. Ltd., The other chemical reagents were purchased from Sinopharm Chemical Reagent Co. Ltd.. All the chemical reagents used here were analytical grade without further purification.

1.2 Synthesis of amorphous red phosphorus

In a typical experiment, 8 g of white phosphorus is added to 100 mL of EDA with continuous stirring to form the homogenous solution. 5 mL of the solution is transferred into 50 mL distilled water to get reddish brown precipitates. The precipitate is washed with ethanol, hydrochloric acid and distilled water successively until the pH value reaches 7 and collected by centrifugation, vacuum freeze drying for

24 h. The reddish brown amorphous red phosphorus is obtained

1.3 Synthesis of amorphous phosphorus spheres

1.5 g of white phosphorus is put into 50 mL of hexamethyldiamine without stir, then reactants are transferred to oven and heated at 50°C for 24 hours. After that, the upper liquid is poured out and the precipitation is obtained. The precipitates are washed with ethanol, carbon disulfide, hydrochloric acid and distilled water successively until the pH value reaches 7 and collected by centrifugation. The amorphous phosphorus spheres are prepared.

1.4 Synthesis of black phosphorus

1.5 g of white phosphorus and 40 mL of hexamethyldiamine are transferred into a 50 mL autoclave with the protection of argon and heated at 200 °C for 12 hours. After cooling down to about 50 °C naturally, the upper liquid is poured out and the black products are collected by centrifugation, and followed by washing with ethanol, carbon disulfide, hydrochloric acid and deionized water respectively. The black phosphorus is obtained.

Structure characterizations

The samples were measured by X-ray diffraction (XRD), which was carried out on a Philips X' Pert Super diffractometer with Cu K α ($\lambda=1.54182 \text{ \AA}$), and Raman spectroscopy was performed by a JYLABRAM-HR Confocal Laser Micro-Raman spectrometer at 532

nm. The morphologies of the samples were characterized on scanning electron microscopy (SEM, JEOL-JSM-6700F) and transmission electron microscopy (TEM, Hitachi H7650). Thermogravimetric analysis (TGA, Shimadzu TGA-50 H) was measured at a heating rate of 10 °C/min from 40 °C to 800 °C under Nitrogen atmosphere to determine the weight of phosphorus. X-ray photoelectron spectroscopy (XPS) data were recorded on an ESCALAB 250 X-ray photoelectron spectrometer (Perkin-Elmer) to characterize the surface composition. High resolution transmission electron microscopy (HRTEM) images were collected on JEM-2100F transmission electron microscope with an accelerating voltage of 200 kV. The Brunauer-Emmett-Teller (BET) surface area and pore distribution were carried out using a BELSORP-max machine, BEL, Japan. The element distribution and lattice fringe were analyzed by energy dispersive x-ray spectroscopy (EDS, JEMARM 200F) and selected area electron diffraction (SAED, JEM-ARM 200F). The FTIR spectra were tested on Fourier transformed infrared spectrometer (FTIR, Hyperion 3000). The ³¹P NMR spectrum was tested on NMR spectrometer (Bruker AVANCE AV III 400) ([D₆] DMSO, 25°C, 242.96 MHz). ³¹P chemical shifts are referenced relative to a solution of 85% H₃PO₄.

The electrochemical properties were measured using coin-type 2016 cells, which were assembled in the argon-filled glove box (O_2 , $H_2O < 0.1$ ppm). Before preparing negative electrode, the active materials (40 wt%) and carbon black (40 wt%) were ball-milled for 12 hours to improve the electrochemical contact. The slurry mixed with as-milled active materials (40 wt%), conductive carbon black (40 wt%) and CMC sodium (20 wt%) in distilled water was coated on a copper foil and dried at 60 °C for 24 h in a vacuum oven. For LIBs test, lithium foil was served as the counter electrode, a solution of 1 M $LiPF_6$ in a mixture of ethylene carbonate / dimethylcarbonate (EC/DMC; 1:1 by volume) with 5 wt% fluoroethylene carbonate(FEC) was used as the electrolyte (Zhuhai Smoothway Electronic Materials Co., Ltd (China)) and Celgard 2400 membrane was applied for a separator. For KIBs test, potassium foil was served as the counter electrode, a Whatman GF/A glass fiber was used as the separator, and a solution of 0.8 M KPF_6 dissolved in ethylene carbonate and propylene carbonate (EC/PC; 1:1 by volume) was employed as the electrolyte. The active material density of each electrode was measured to be about 0.4-0.6 mg cm^{-2} . The galvanostatic charge/discharge properties were tested on a battery tester (LANDCT2001A) at different current densities in a voltage window of 0.01-2.5V. The cyclic voltammogram (CV)

measurements were collected on a CHI660D Electrochemical Workstation. The data of conductivity was collected by conductivity meter, the electrode in the electrolytic cell is Platinized Platinum Electrode (Leici DDSJ-318; Shanghai).



Figure S1. The photographs of the precipitation process.

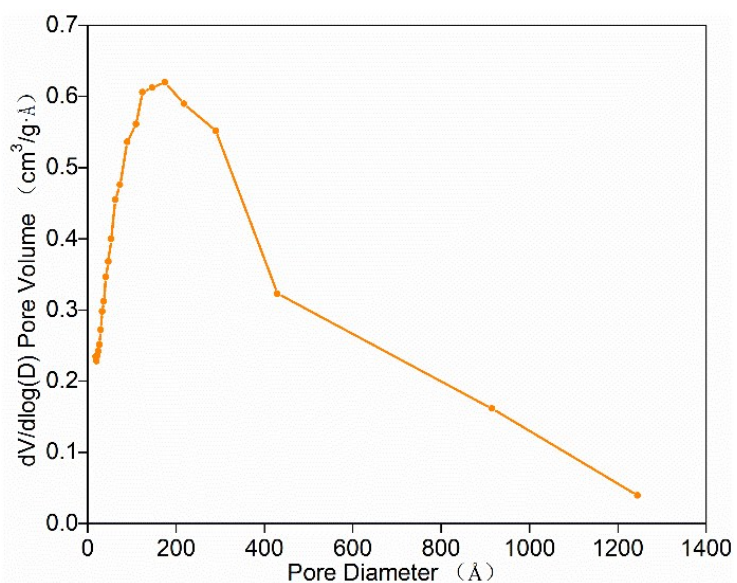


Figure S2. The pore size distribution of the amorphous red phosphorus nanoparticles.

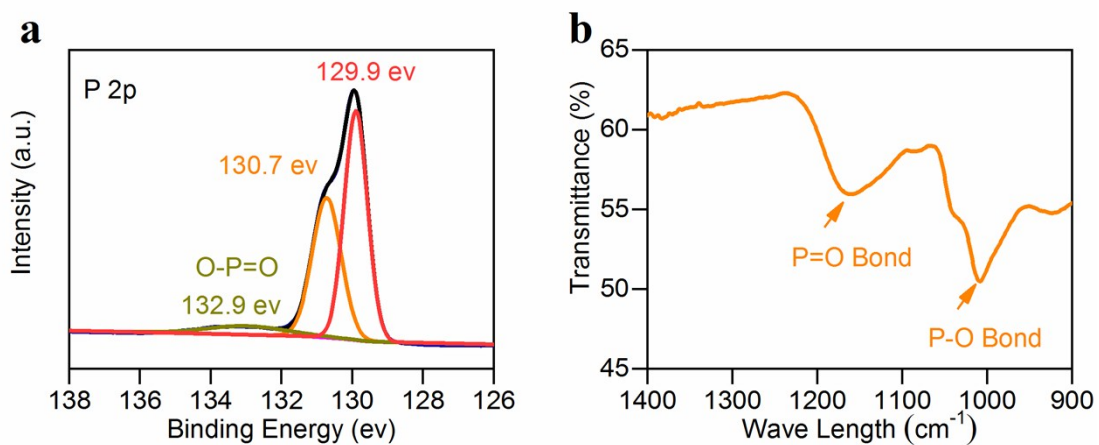


Figure S3. The XPS P2p spectra and the FTIR spectrum of the as-prepared phosphorus

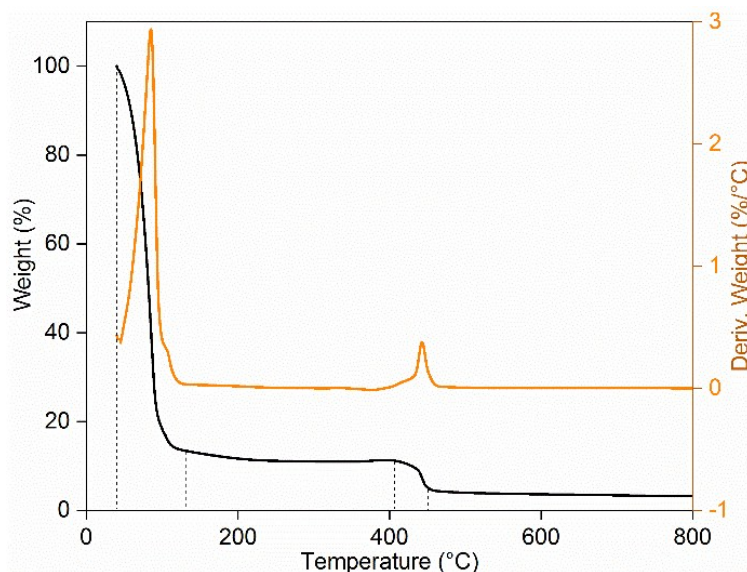


Figure S4. The TGA curve of HM under N₂.

Figure S4 displays an apparent two-step process in the range of 40–800 °C under N₂ atmosphere. From 40 °C to 128.5 °C, mass loss is due to the gradual evaporation of EDA and absorbed moisture, while the weight loss between 407.4 °C and 459.1 °C is contributed to the result of phosphorous sublimation.

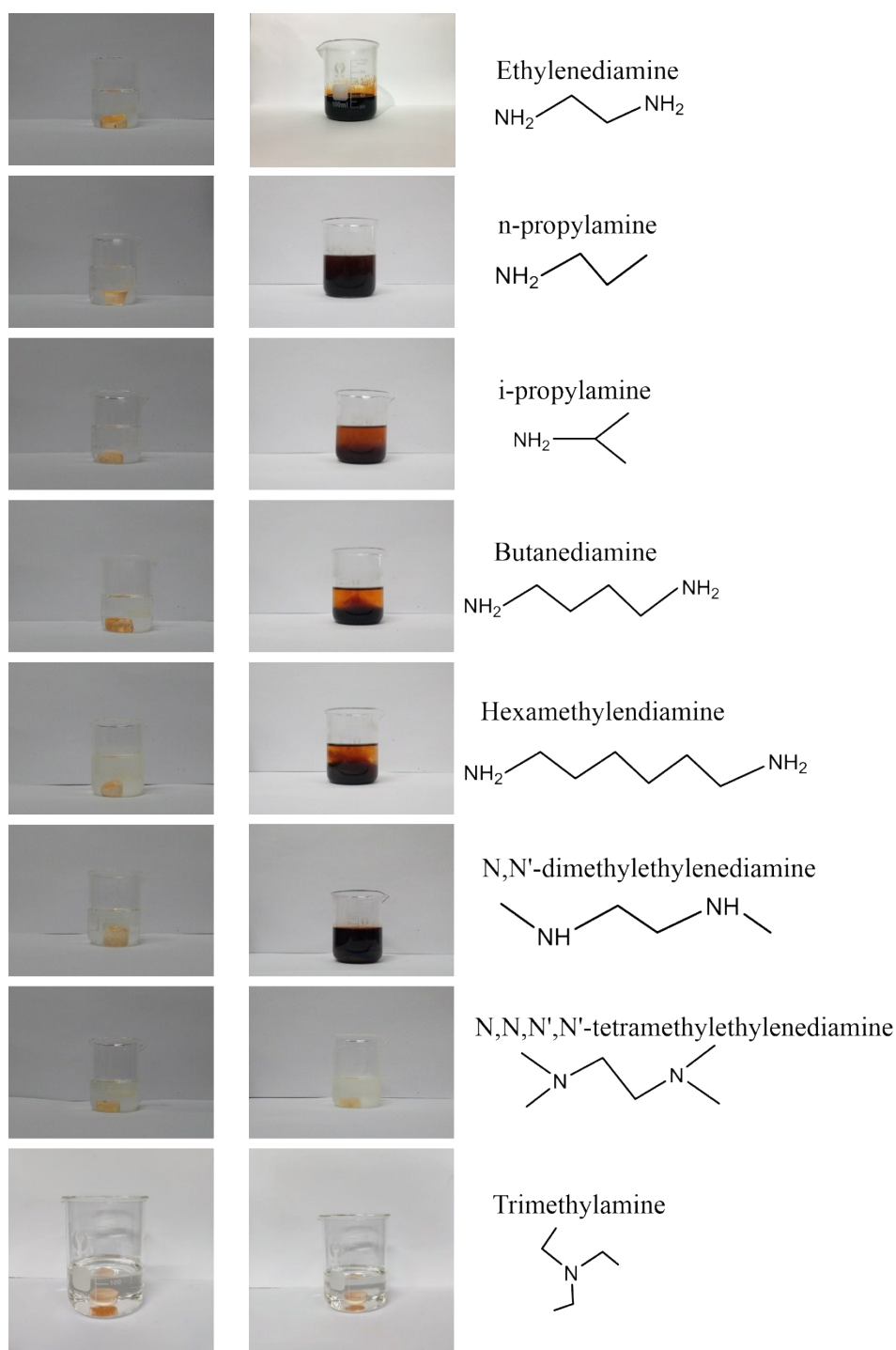


Figure S5. The digital pictures of reaction process of various amines.

As shown, only primary amine and secondary amine reacted with white phosphorus, while white phosphorus was put into tertiary amine such as N,N,N',N'-tetramethylethylenediamine and trimethylamine, there was no obvious change happened.

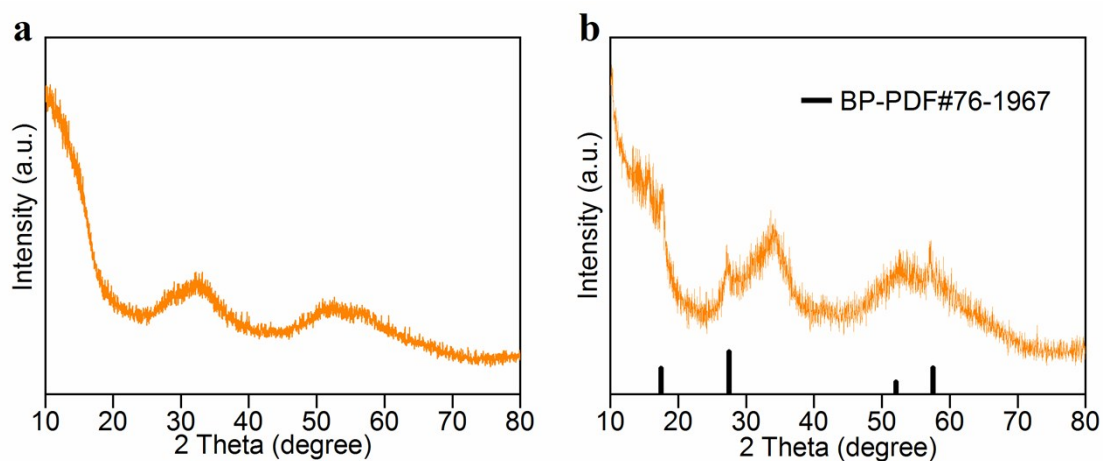


Figure S6 The XRD patterns of red phosphorus spheres and black phosphorus.

Two broad diffraction peaks at 23-40° and 47-70° also prove the amorphous property of sample. **Fig S6 (b)** further confirms that amorphous red phosphorus and black phosphorus synchronously exist in the sample.

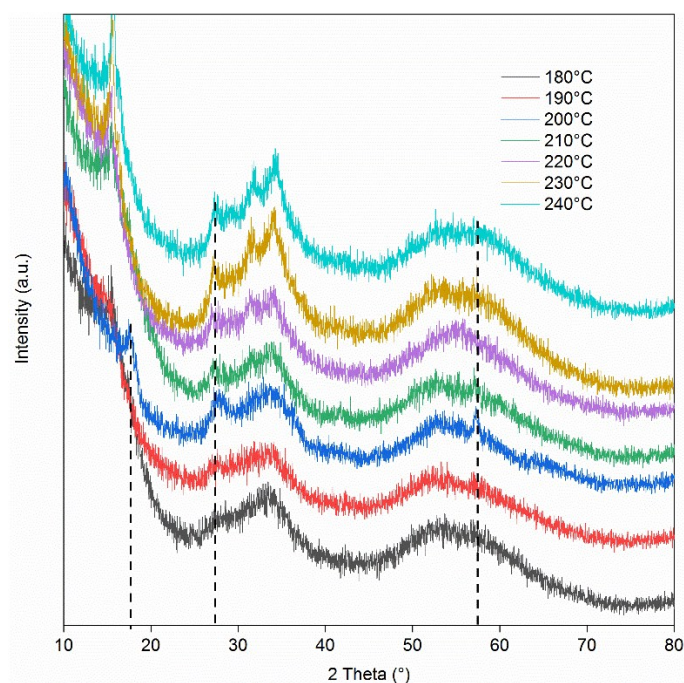


Figure S7 The relationship between product and temperature in WP/hexamethylenediamine.

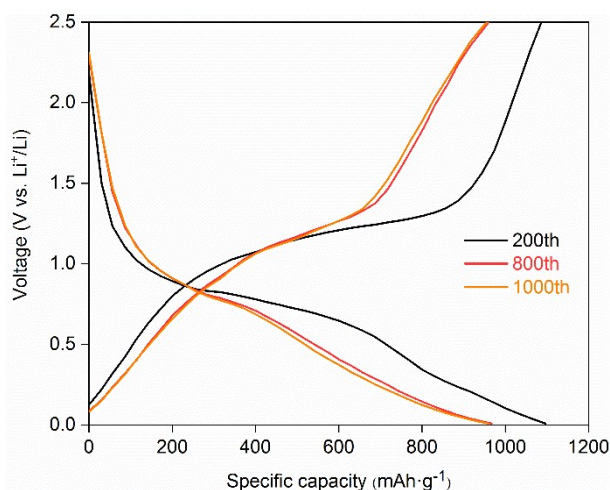


Figure S8 The charge-discharge curves of 200th, 800th, 1000th.

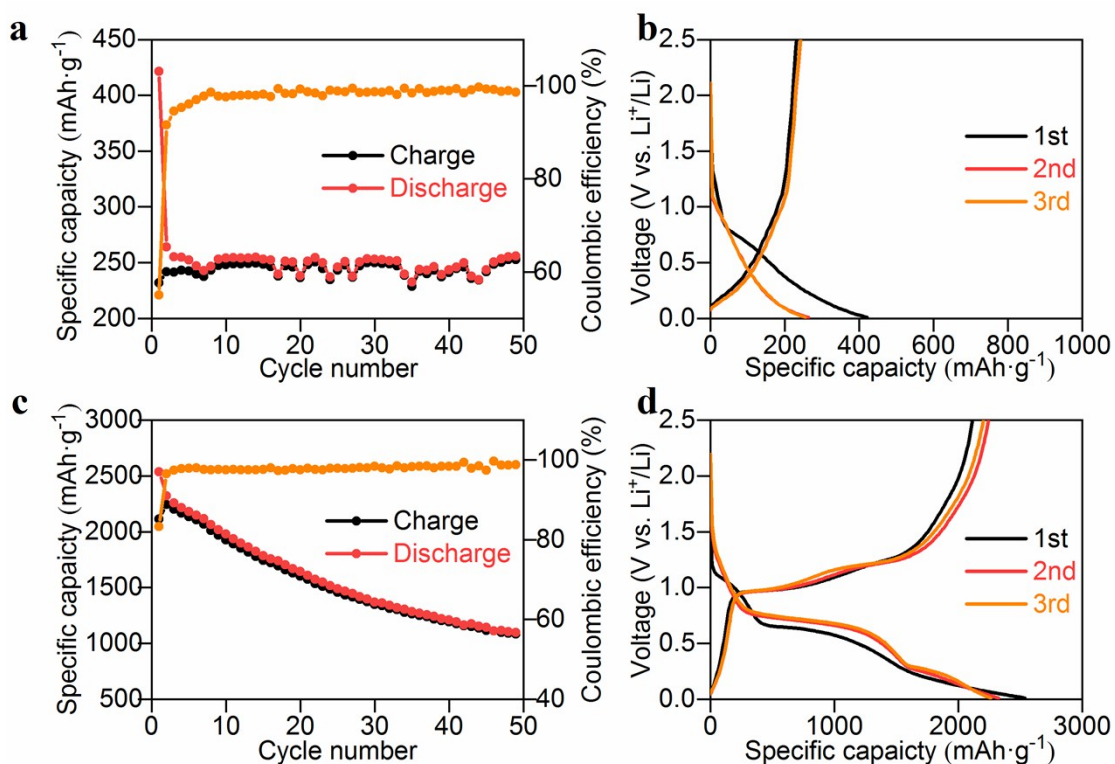


Figure S9 The electrochemical properties of the red phosphorus spheres (a,b) and black phosphorus in LIBs (c,d) at 400 mA g⁻¹.

As a contrast, the electrochemical properties of amorphous red phosphorus spheres and as-prepared black phosphorus were also studied. Due to the micrometer grade of size and low specific surface area (0.8048 m² g⁻¹, **Fig. S10**) of red phosphorus spheres,

which hinder the lithiation process. The electrochemical performance of the as-prepared black phosphorus is better than sphere-like red phosphorus but worse than amorphous phosphorus nanoparticles. The initial Coulombic efficiency of black phosphorus was up to 83.31% while the capacity retention was poor. Low surface area ($66.31 \text{ m}^2 \text{ g}^{-1}$, as shown in **Fig. S10**) and relatively high conductivity accounted for the upward initial Coulombic efficiency. However, the large size of material led to the decrease of cycle stability, the volume expansion is the main problem of P-based anode.

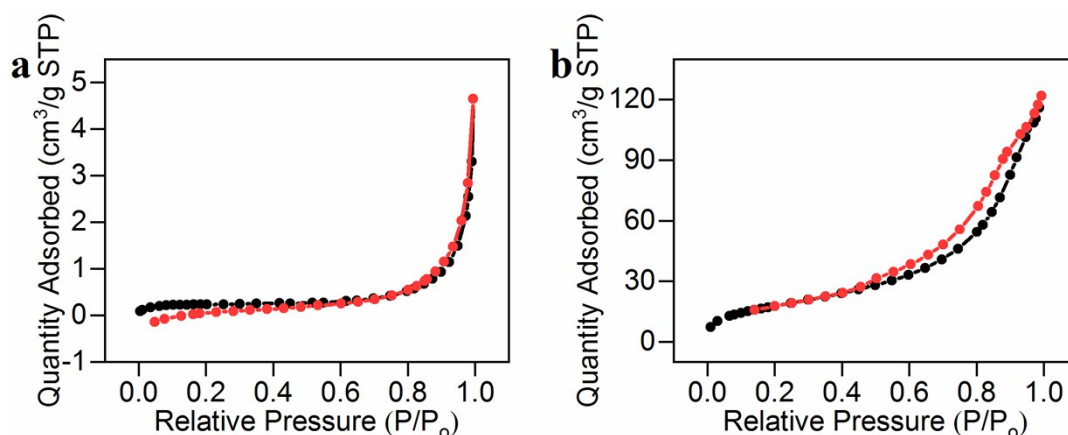


Figure S10 The Nitrogen adsorption-desorption isotherms of the red phosphorus spheres and black phosphorus.

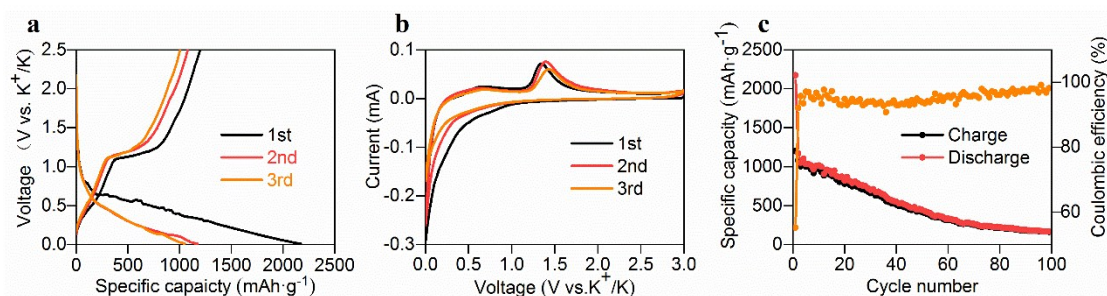


Figure S11 The electrochemical properties of the amorphous red phosphorus anode for KIBs

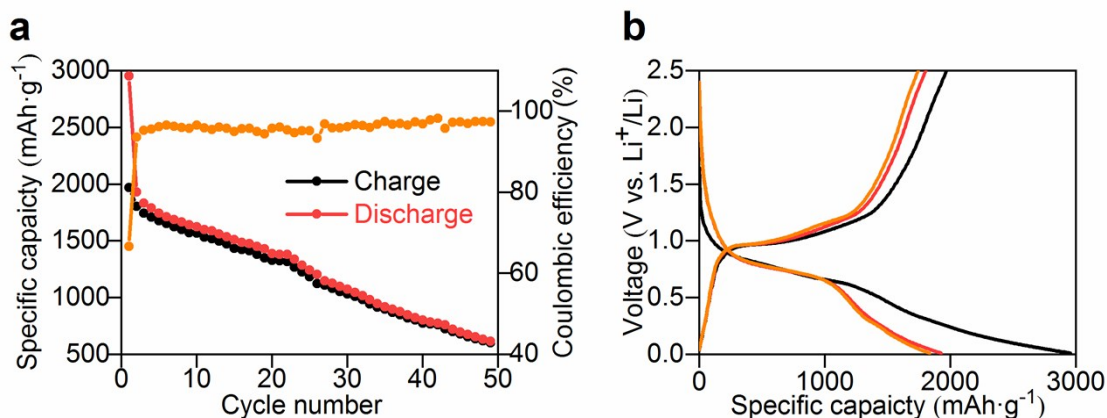


Figure S12 The electrochemical properties of the amorphous red phosphorus anode for LIBs with the proportion of composition: active materials (60 wt%), conductive carbon black (20 wt%) and CMC sodium (20 wt%)

Besides, increasing conductive carbon black content would improve the initial Coulombic efficiency and the stability, as shown in **Fig. S12**. The above data indicates that the types of phosphorus are not the most significant factor while nano-treatment of phosphorus and raising the electrical conductivity are more important for P-based material as anodes for lithium-ion batteries.

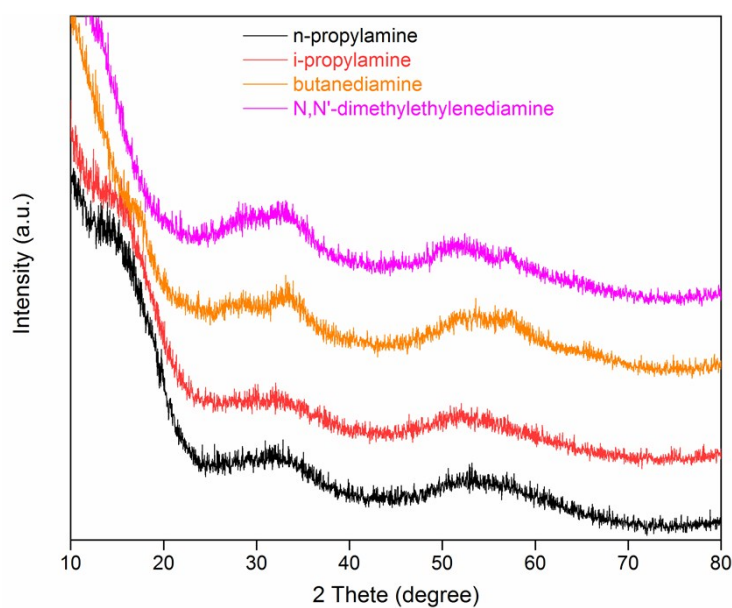


Figure S14 The XRD patterns of n-propylamine, i-propylamine, butanedi-amine, N,N'-dimethylethylenedi-amine

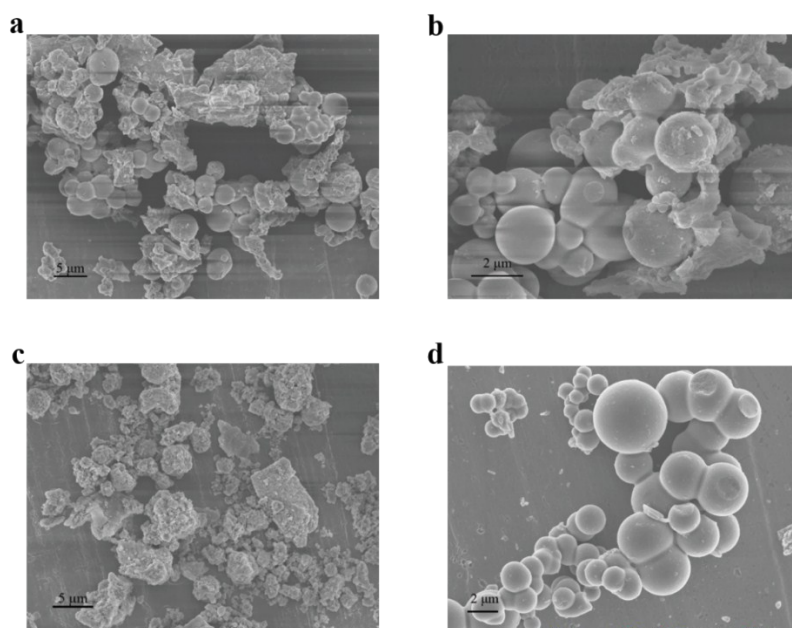


Figure S15 The SEM images of n-propylamine, i-propylamine, butanediamine, N,N'-dimethylethylenediamine

Materials	Cycling Stability (n cycles)	Rate Performance	Reference
Black Phosphorus-Graphite	0.52 A·g ⁻¹ , n=100, 1840 mAh g ⁻¹	11.7 A·g ⁻¹ , 1240 mAh g ⁻¹	1
Phosphorus-based nanosheets	0.2 A·g ⁻¹ , n=100, 1683 mAh g ⁻¹	20 A·g ⁻¹ , 630 mAh g ⁻¹	2
Red phosphorus/graphene	0.2 A·g ⁻¹ , n=100, 1286 mAh g ⁻¹	10 A·g ⁻¹ , 873 mAh g ⁻¹	3
Red phosphorus/CNFs	0.26 A·g ⁻¹ , n=100, 2030 mAh g ⁻¹	28.6 A·g ⁻¹ , 380 mAh g ⁻¹	4
Red phosphorus/CNTs	0.1 A·g ⁻¹ , n=1000, 1400 mAh g ⁻¹	2 A·g ⁻¹ , 800 mAh g ⁻¹	5
Amorphous phosphorus	1.5 A·g ⁻¹ , n=1000, 955.5 mAh g ⁻¹	20 A·g ⁻¹ , 1210.2 mAh g ⁻¹	Our work

Table S1 Comparisons with other P based anode materials for LIBs reported in literature

References

1. J. Sun, G. Zheng, H.-W. Lee, N. Liu, H. Wang, H. Yao, W. Yang and Y. Cui, *Nano letters*, 2014, 14, 4573-4580.
2. Y. Zhang, X. Rui, Y. Tang, Y. Liu, J. Wei, S. Chen, W. R. Leow, W. Li, Y. Liu and J. Deng, *Advanced Energy Materials*, 2016, 6, 1502409.
3. L. Sun, Y. Zhang, D. Zhang and Y. Zhang, *Nanoscale*, 2017, 9, 18552-18560.
4. W. Li, Z. Yang, Y. Jiang, Z. Yu, L. Gu and Y. Yu, *Carbon*, 2014, 78, 455-462.
5. T. Yuan, J. Ruan, C. Peng, H. Sun, Y. Pang, J. Yang, Z.-F. Ma and S. Zheng, *Energy Storage Materials*, 2018, 13, 267-273.